Competition between terminating and collective structures above spin 40$\hbar$ in ^{154}Dy

W. C. Ma,[1] R. V. F. Janssens,[2] T. L. Khoo,[2] I. Ragnarsson,[3] M. A. Riley,[4] M. P. Carpenter,[2] J. R. Terry,[1] J. P. Zhang,[1] I. Ahmad,[2] P. Bhattacharyya,[5] P. J. Daly,[5] S. M. Fischer,[2] J. H. Hamilton,[6] T. Lauritsen,[2] D. T. Nisius,[2] A. V. Ramayya,[6] R. K. Vadapalli,[1] P. G. Varmette,[1] J. W. Watson,[1] C. T. Zhang,[5] and S. J. Zhu[1,*]

[1]*Department of Physics, Mississippi State University, Mississippi State, Mississippi 39762*

[2]*Argonne National Laboratory, Argonne, Illinois 60439*

[3]*Department of Mathematical Physics, Lund Institute of Technology, S-22100 Lund, Sweden*

[4]*Department of Physics, Florida State University, Tallahassee, Florida 32306*

[5]*Department of Chemistry, Purdue University, West Lafayette, Indiana 47907*

[6]*Department of Physics, Vanderbilt University, Nashville, Tennessee 37235*

(Received 12 October 2001; published 21 February 2002)

High-spin states in ^{154}Dy were studied with the Gammasphere spectrometer using the ^{36}S(^{122}Sn,4n) reaction. Band terminating states were identified in the spin range $I=(36-48)\hbar$, and were found to compete with collective rotational cascades up to the highest observed spins. Several ''sidebands'' feeding the terminating structures were identified as well. A band dominated by $M1$ transitions was observed to terminate at $I^{\pi}=42^{-}$. The data are interpreted within the framework of configuration-dependent cranked Nilsson-Strutinsky calculations without pairing.

DOI: 10.1103/PhysRevC.65.034312 PACS number(s): 21.10.Re, 23.20.Lv, 27.70.+q, 21.60.Ev

I. INTRODUCTION

Transitional nuclei such as ^{154}Dy with 66 protons and 88 neutrons, e.g., with a small number of nucleons outside the $Z=64$ and $N=82$ shells, are ideally suited to investigate the microscopic origin of collective rotation, its evolution with rotational frequency, and the impact of structural changes at high spin on global nuclear properties such as the shape. These nuclei are prolate in their ground state and, hence, they are susceptible to rotation. Rotation is a collective phenomenon, but from a microscopic point of view, the angular momentum is built from the many small contributions of the spins of the valence particles. As the total angular momentum increases, the valence spins become more and more aligned along the rotation axis. Once the individual spins of all the valence nucleons in a configuration are fully aligned, i.e., once they are quantized along the rotation axis, the so-called terminating state has been reached [1,2]. As several of the valence nucleons occupy high-j orbitals, large spin values can be achieved in this way. In addition, the matter distribution of these aligned particles is oblate. Thus, as a function of rotational frequency, a gradual change will occur from a collective prolate to a noncollective oblate shape. In ^{154}Dy, structures associated with this gradual alignment process (usually referred to as band termination) have been identified along the zero-temperature yrast line at spin 36^{+}, and suggested for higher spins in both positive- and negative-parity configurations [3–5]. In addition, a prolate to oblate phase transition at higher temperatures has been investigated previously through a study of quasicontinuum γ rays [6].

In the present work, band terminations have been delineated in great detail in the $I=(40-50)\hbar$ domain, i.e., it has been possible to study the dependence of the phenomenon on the configuration involved. At the same time, band sequences that maintain their rotational character have also been traced to similar spin values. Thus, this data set provides the opportunity to study the configuration dependence of collective and single-particle degrees of freedom at high spin and to compare the experimental results with state-of-the-art mean-field calculations.

II. EXPERIMENTAL AND DATA ANALYSIS PROCEDURES

The experiment was performed at the 88-in. cyclotron at the Lawrence Berkeley National Laboratory. Excited states in ^{154}Dy were populated via the ^{36}S(^{122}Sn,4n) reaction at 165 MeV. The target consisted of a stack of three 330 μg/cm^2 isotopically enriched, self-supporting foils. Decay γ rays were detected with the Gammasphere spectrometer [7], which consisted of 103 Compton-suppressed Ge detectors. A total of 1.5×10^9 events was collected with five or more suppressed Ge detectors required to fire in prompt coincidence.

The data were sorted into three-dimensional histograms (cubes) gated either on the measured multiplicity or on the strongest yrast ^{154}Dy transitions. The analysis was carried out with the Radware software package [8]. The level scheme presented in Fig. 1 was constructed mostly from γ-ray coincidence relationships, with additional support from the observation of cascade-crossover transitions and intensity considerations. The spin and parity assignments of Fig. 1 were based on γ-ray multipolarities derived using the measured DCO (directional correlation of oriented nuclei) ratios [9]. The latter were obtained from an angle-sorted asymmetric cube where γ rays detected at forward ($\leqslant37.4°$) and backward ($\geqslant142.6°$) angles were placed on the X axis, those measured at sideward angles (between 69.8° and 110.2°) on the Y axis, and those measured at any angle with respect to the beam direction on the Z axis. This DCO cube was ana-

*On leave from Department of Physics, Tsinghua University, Beijing 100084, China.

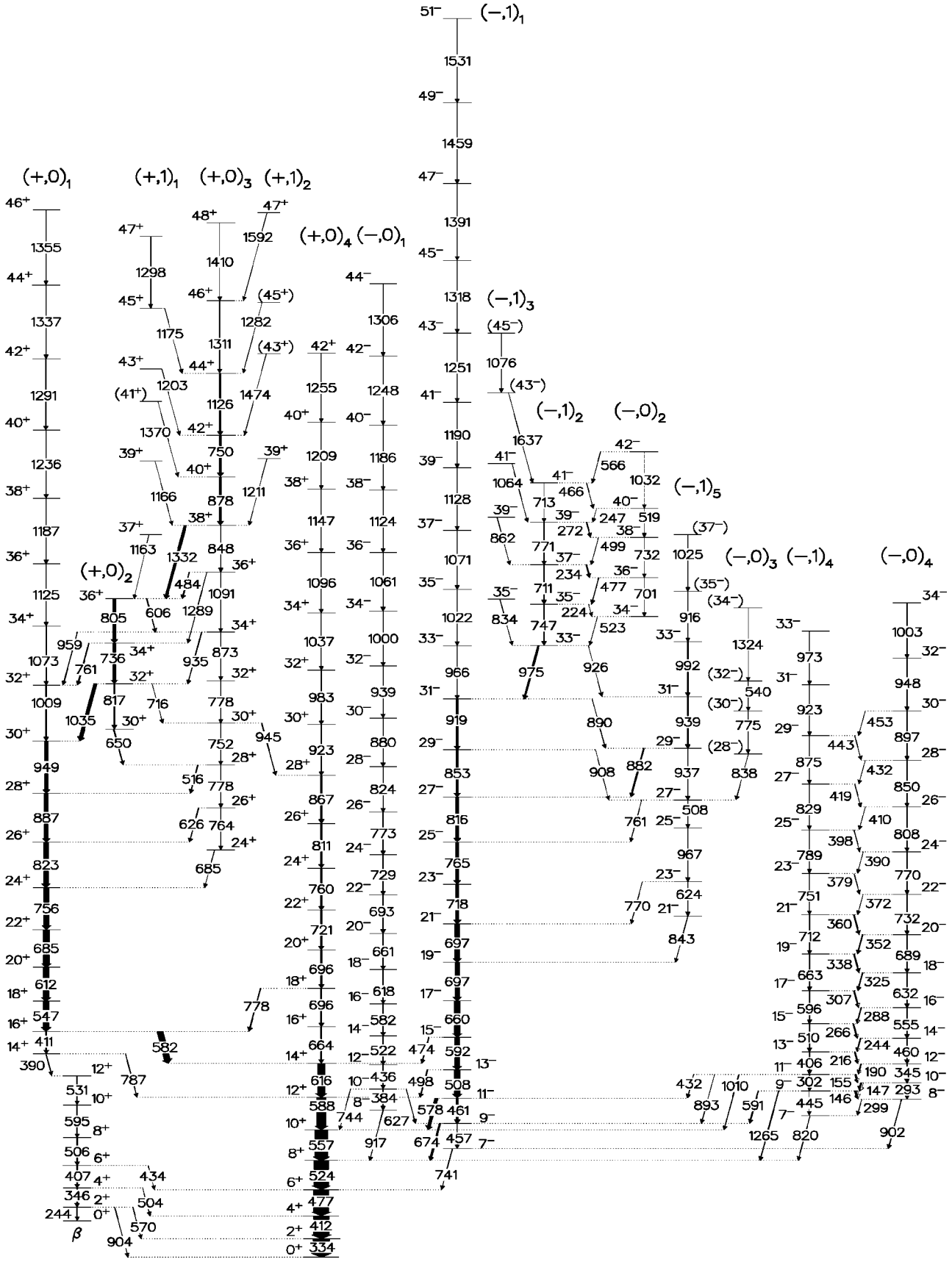

FIG. 1. ^{154}Dy level scheme from this work. The γ-ray intensities are indicated by the arrow widths, and the decay sequences are labeled by the parity and the signature (π,α).

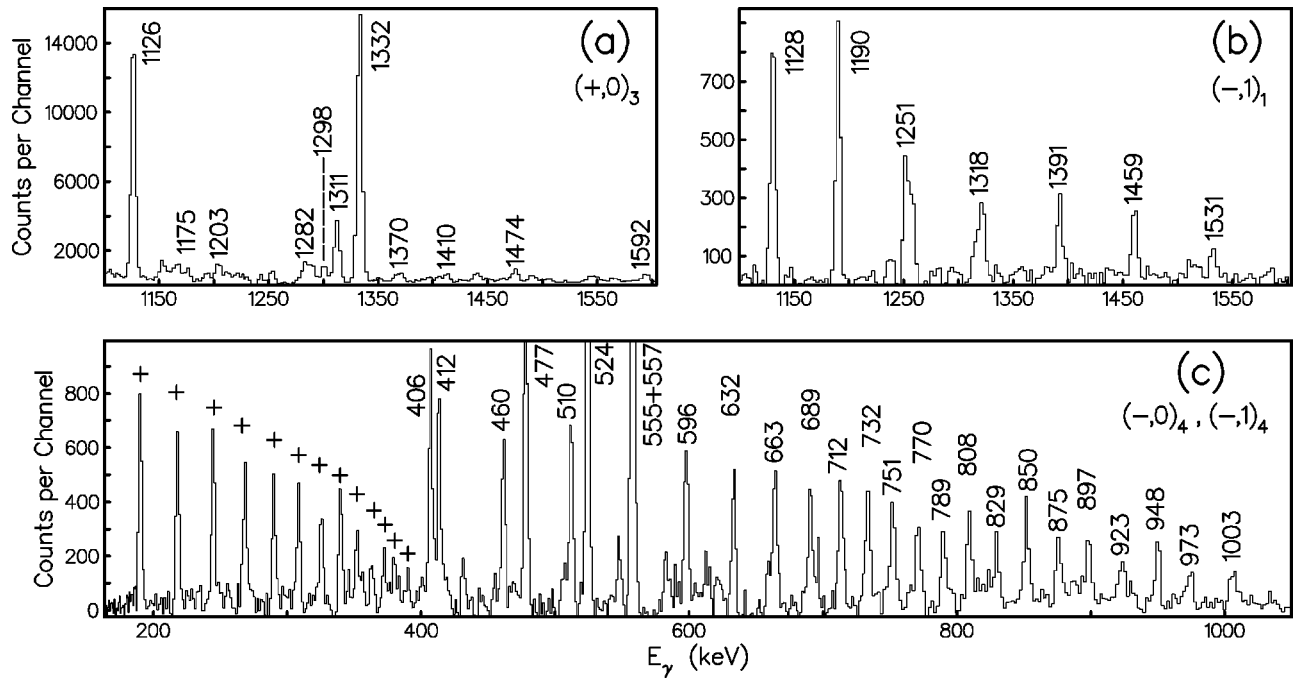

FIG. 2. (a) Coincidence spectrum double gated on γ-ray transitions along the strongest decay pathway between the 42^+ state of band $(+,0)_3$ and the 30^+ state of band $(+,0)_1$ showing the abrupt band termination at high spins. Side-feeding transitions for this band are also marked by their energies. (b) High-spin region of a coincidence spectrum for band $(-,1)_1$ double gated on the transitions between the 49^- and 31^- levels. (c) Coincidence spectrum of bands $(-,0)_4$ and $(-,1)_4$ double gated on the 1010-keV decay-out transition and any one of the $M1$ transitions, marked with the "+" symbol, between the 11^- and 24^- levels. The spectra were extracted from a cube gated by the lowest four yrast transitions.

lyzed with the XMII program [10] and the technique was calibrated with strong transitions of known multipolarity. The extracted DCO ratios fall into two distinct groups centered around 1.0 and 0.6 for stretched quadrupole and dipole transitions, respectively.

III. EXPERIMENTAL RESULTS

Most bands established earlier [3,4] have been extended here to higher spins and, in several instances, placements and orderings were altered substantially, e.g., in band $(+,0)_4$ above the 18^+ level, in band $(-,1)_1$ above 27^-, and in bands $(-,0)_2$ and $(-,1)_2$. Bands $(-,0)_1$, $(-,0)_4$, and $(-,1)_4$ (Fig. 1) as well as other short sequences have been observed for the first time. Band $(+,0)_1$ was known up to the 32^+ level, where it looses its yrast status. This band has now been extended to 46^+ through a rotational cascade of weak transitions with energies greater than 1 MeV. At low spin, a new, weak deexcitation path (390 keV) to an extended β-vibrational band has been identified. Band $(-,1)_1$ has been clearly delineated from 33^- to 51^-, the level with the highest spin and excitation energy reported here. A spectrum illustrating the top of the cascade is given in Fig. 2. One of the prominent level sequences of positive parity is band $(+,0)_3$, which collects a large fraction of the flux in the spin region above $36\hbar$. Remarkably, the γ-ray intensity drops quickly at the highest spins: while the 1126-keV $44^+ \rightarrow 42^+$ transition carries 9.5% of the intensity of the $2^+ \rightarrow 0^+$ ground state transition, the 1311- and 1410-keV γ rays located just above it drop to 3.2% and 0.4%, respectively. This is due to the large fragmentation of the decay pathways that is noticeable along this sequence. Nevertheless, the band has now been observed up to its expected termination (see discussion below), hereby removing an ambiguity remaining from the study of Ref. [4]. A spectrum of this band is also shown in Fig. 2. Several additional weak transitions feeding this band between the 36^+ and 46^+ states were found to be of stretched dipole character. Therefore, they depopulate levels with odd spins. These have been tentatively grouped into the two sequences labeled $(+,1)_1$ and $(+,1)_2$. Positive parity is proposed for the latter sequences because of their close connection with band $(+,0)_3$, which is reflected in the absence of in-band $E2$ transitions (with the exception of the 1298-keV γ ray) indicating that the associated transition probabilities must be smaller than those for the decay-out towards band $(+,0)_3$. The situation in band $(-,1)_2$ is similar to that in band $(+,0)_3$: this structure collects a larger fraction of the γ-ray flux in this spin region than any other, except for band $(+,0)_3$. However, the band terminates at the 41^- state with a very weak 713-keV transition. Its unfavored signature partner, band $(-,0)_2$, is of much weaker intensity. Five levels were tentatively grouped together in a band labeled $(-,1)_3$. Three linking transitions between these states and band $(-,1)_2$ were measured to have stretched $E2$ character. Similar to bands $(+,1)_1$ and $(+,1)_2$, no in-band $E2$ transition was observed, except for the 1076-keV γ ray.

Like band $(+,0)_1$, bands $(+,0)_4$, $(-,0)_1$, and $(-,1)_1$ maintain their rotational character up to the highest spins.

The ground state band, $(+,0)_4$, is crossed at 14^+ by the s band, $(+,0)_1$, associated with a first pair of aligned $i_{13/2}$ neutrons [3,4]. Band $(-,0)_1$ is new to this work. Despite a maximum intensity of only $\sim 5\%$, it was traced up to 44^-. The strongest decay path out of this band proceeds via a 627-keV stretched dipole transition depopulating the 3048-keV level to the 9^- state in band $(-,1)_1$. This 3048-keV level was assigned as 10^- based on the following arguments: (i) a 10^+ possibility was ruled out because of the absence of the $10^+ \rightarrow 8^+$ and $8^+ \rightarrow 6^+$ transitions that would be expected to link bands $(-,0)_1$ and $(+,0)_4$, (ii) similar considerations rule out a 8^+ assignment, while (iii) a 8^- hypothesis would require an unlikely $M2$ character for the 744- and 917-keV transitions. In addition, the band can be interpreted as the signature partner of band $(-,1)_1$ in view of the striking similarities in their respective moments of inertia and alignments. Spin and parity assignments to low-spin levels in the strongly coupled bands, $(-,0)_4$ and $(-,1)_4$ shown in Fig. 2(c), are based mainly on the stretched dipole character of the strongest decay-out transition, the 1010-keV γ ray depopulating the 3314-keV state towards the ground state band. An $I=9\hbar$ assignment to this level is ruled out as it would require the 820-keV γ ray to be associated with an unlikely $\Delta I=3\hbar$ transition. An 11^+ assignment is not possible either as it implies that a 893-keV $M2$ transition would be sharing decay-out flux with 1010- and 432-keV dipole transitions. Therefore, this level was assigned the quantum numbers 11^-. Finally, band $(-,1)_5$, which was delineated from 21^- to a level tentatively assigned as 37^-, is characterized by irregular transition energies, a feature also displayed by the short feeding sequence constituting band $(-,0)_3$. These last two bands are given here for completeness. Their nature is at present unclear and they will not be discussed hereafter.

IV. DISCUSSION

In Ref. [3], calculations within the configuration-dependent cranked Nilsson-Strutinsky (CNS) approach [2,11] had been used to predict many of the band structures discovered in the present work. The same approach is employed here, but the calculations differ from the earlier ones in several aspects. A modified $A=150$ parameter set (e.g., [12,13]) was introduced, which differs from the standard one [11] in its larger $Z=64$ shell gap, and in the energy degeneracy of the $g_{7/2}$ and $d_{5/2}$ proton subshells.[1] In addition, with the new computer codes, it is not only possible to fix the distribution of the particles over the N shells (or more precisely, the N_{rot} shells), but also to fix the distribution between orbitals dominated by the high-j intruder and the other j components of a single N shell [14]. This makes it possible to specify, for example, the distribution of neutrons over the $h_{11/2}$ and the other $N=5$ subshells (mainly $h_{9/2}f_{7/2}$ for $N \approx 90$). Furthermore, in specific cases, it was possible to specify further the occupation of orbitals dominated by specific j shells and to track, for example, the number of protons excited from orbitals of $(g_{7/2}d_{5/2})$ character below the $Z=64$ gap to configurations of $(d_{3/2}s_{1/2})$ character above this gap [15]. It is worth keeping in mind that the CNS approach neglects pairing and, as a result, calculations become realistic only at fairly high spin, e.g., $I \geqslant (25-30)\hbar$.

The calculated configurations are labeled as $[p_1p_2(p_3p_4),(n_0)n_1n_2]$, where p_1 is the number of proton holes of $(g_{7/2}d_{5/2})$ character, p_2 is the number of $h_{11/2}$ protons, n_1 is the number of $h_{11/2}$ neutron holes, and n_2 is the number of $i_{13/2}$ neutrons. Furthermore, the labels in parentheses, given only when they are different from zero, denote the number of $(h_{9/2}f_{7/2})$ (p_3) and $i_{13/2}$ (p_4) protons, and $N=4$ neutron holes (n_0), respectively. The number of $(d_{3/2}s_{1/2})$ protons and $(h_{9/2}f_{7/2})$ neutrons is not given explicitly, but can be determined from the total number of nucleons.

A. Rotational bands

Judging from their energy sequences, bands $(+,0)_1$, $(+,0)_4$, $(-,0)_1$, $(-,1)_1$, $(-,0)_4$, and $(-,1)_4$ appear to maintain their rotational character up to the highest spins. For the three strongest among them, this is supported by lifetime measurements [4,5], which, unfortunately, do not extend into the spin domain where they are relevant for configuration assignments. The six bands are drawn vs a rigid rotation reference in Fig. 3, where they are also compared with selected calculated configurations. As indicated above, band $(-,1)_1$ is observed to be regular all the way up to $I=51^-$. Contrary to the assumptions in [3], the present calculations indicate that neutron $h_{11/2}$ holes have to be involved. In the absence of such holes in the configuration, maximum achievable spins are only slightly above $50\hbar$ and the calculated bands all show clear signs of approaching termination below this $50\hbar$ spin value. Configurations with a single $h_{11/2}$ hole result in signature degenerate bands, contrary to the observed $(-,1)_1$ band. Thus, this band must be assigned to a configuration with two $h_{11/2}$ neutron holes, and the possible configurations are then [46,23], drawn in Fig. 3, and [45,22]. The latter is calculated to lie a few hundred keV higher in energy. Considering this energy difference and the general features of the $\nu(h_{11/2})^{-2}$ excitations discussed below, a [46,23] assignment appears to be the only realistic one.

The fact that band $(-,0)_1$ can be interpreted as the signature partner of band $(-,1)_1$, as stated above, can be inferred in Fig. 3 from the parallel trajectories in the energy vs spin plane. Hence, the two bands have the same distribution of the particles over the j shells, i.e., a [46,23] configuration, but with an opposite signature for the fifth $(h_{9/2}f_{7/2})$ neutron. Furthermore, the even spin positive-parity configuration with one neutron moved from the $i_{13/2}$ orbit to the $(h_{9/2}f_{7/2})$ configuration, [46,22], is calculated to lie low in energy for $I=(20-40)\hbar$ and reproduces the observed band $(+,0)_1$ quite well (Fig. 3). Note that the [46,22] band is calculated to cross the [46,23] bands in the $I=(40-50)\hbar$ region, in agreement with experiment. It is worth noting that these three bands have the same distribution of the 8 $(h_{9/2}g_{7/2})$ and $i_{13/2}$ neu-

[1] In Ref. [11], the $Z=64$ gap was simulated by shifting the bands by an amount depending on their $\pi h_{11/2}$ content and the $g_{7/2}$ subshell was ~ 0.5 MeV below the $d_{5/2}$ one.

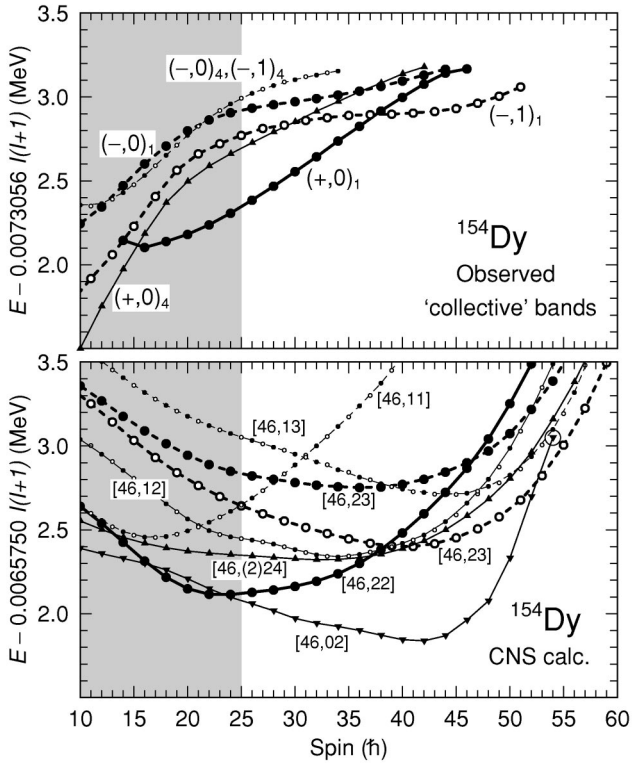

FIG. 3. Observed (upper panel) and calculated (lower panel) collective bands in ^{154}Dy. The CNS calculations are done without pairing, thus they apply only at high spin, above the shaded region. The observed bands are plotted versus the standard $kI(I+1)$ of Ref. [2], i.e., with the constant k chosen to equal 0.007 MeV for $A=158$ and scaled with $A^{-5/3}$. As noted previously for the neighboring nucleus ^{155}Dy [16], one discrepancy often found between calculations and experiment is that the average energy cost per spin unit is somewhat higher for the observed bands than for the calculated bands. Thus, in order to get similar slopes in the theory panels of the figure, the subtracted reference energy is 10% smaller for the calculated than for the experimental ones. The observed bands interpreted as having two $h_{11/2}$ neutron holes in their configurations and their calculated counterparts are drawn by thick lines and large symbols. The interpretation of the other bands drawn with thinner lines is more tentative as discussed in the text.

trons as the three low-lying bands terminating at 46^+, 48^-, and 49^- in ^{158}Er [13]. Two calculated configurations of Fig. 3, i.e., [46,02] and [46,(2)24], can be viewed as candidates for the description of band $(+,0)_4$. The former configuration terminates high above the yrast line at $I=54$ and is characterized by rather low collectivity, while the latter has two neutron holes in the $N=4$ shell and two in the $h_{11/2}$ orbit, leading to large deformation $(\varepsilon\approx 0.28, \gamma\approx -20°)$. The [46,(2)24] configuration reproduces the general evolution in excitation energy and spin quite well, but an assignment to the [46,02] configuration cannot be entirely ruled out, because it remains difficult to understand why this configuration has not been observed experimentally despite the fact that it is calculated to lie low in excitation energy over a large spin range. Finally, the last two bands, which maintain their rotational character up to the highest observed spins, $(-,0)_4$ and $(-,1)_4$, form a strongly coupled structure where the absence of signature splitting indicates that the associated configuration must contain a high-K orbital. A [505]11/2 neutron hole configuration is proposed, as this $h_{11/2}$ orbital is the only high-K state close to the Fermi surface. The lowest calculated negative-parity $(h_{11/2})^{-1}$ configuration at low spin, [46,11], is assigned. As seen in Fig. 3, the [46,11] band is crossed by the [46,13] configuration around $I=30\hbar$, suggesting an alignment of two $i_{13/2}$ neutrons. The calculation is in general agreement with the data where a crossing appears to take place in the $I=(25-30)\hbar$ range. It should be noted that several other $(h_{11/2})^{-1}$ configurations are calculated to be low in energy at spin values $I=(30-40)\hbar$. One such band, i.e., the one labeled [46,12], has been drawn in Fig. 3.

B. Terminating structures

While the rotational sequences are characterized at spins $I\geqslant 25\hbar$ by flat or upsloping trajectories when drawn vs a rigid rotor reference (Fig. 3), other bands reported here exhibit a marked downslope as can be seen in the upper panel of Fig. 4 (note that the bands connected by $E2$ transitions are drawn with thick lines): this is indicative of structures approaching termination [2]. Calculations for the configurations assigned to the terminating bands are presented in the middle panel of the figure. The calculated bands drawn with thick lines are all associated with configurations of the type $\pi(d_{5/2}g_{7/2})^{-n}(h_{11/2})^{2+n}\nu(h_{9/2}f_{7/2})^4(i_{13/2})^2$ containing $n=0$, 1, and 2 proton holes in the $Z=64$ core. In these configurations, the neutrons and the $h_{11/2}$ protons contribute with their maximum spins of $26\hbar$ and $10\hbar$, $13.5\hbar$, and $16\hbar$, respectively. The spin contribution from the $d_{5/2}g_{7/2}$ proton hole(s) in the energetically most favored states depends on the relative position of these two subshells.

1. Negative-parity levels

Negative-parity states are formed when one proton is excited from $d_{5/2}g_{7/2}$ to $h_{11/2}$. The proton hole can be placed in $m_i=-1/2$, $-3/2$, $-5/2$, or $-7/2$ orbitals leading to configurations with the maximal spin varying from $I=26\hbar+13.5\hbar+0.5\hbar=40\hbar$ up to $I=26\hbar+13.5\hbar+3.5\hbar=43\hbar$. The relative energies of these states can be estimated from an e_i vs m_i diagram, see Fig. 7 of Ref. [17]. The $m_i=-3/2$ and $-5/2$ orbitals are calculated to be most favored energetically leading to the low-lying terminating 41^- and 42^- states associated with the configurations labeled [13,02] in Fig. 4. These two maximaly aligned states provide a natural explanation for the experimental levels of corresponding spin in bands $(-,1)_2$ and $(-,0)_2$. The 40^- level of band $(-,0)_2$ is worth a closer look as its energy is lower than would be expected on the basis of a smooth extrapolation from the γ-ray transition energies between the lower band members. In the calculations, the $m_i=-1/2$ orbital is only slightly less favored in excitation energy than the $m_i=-3/2$ and $-5/2$ ones and, as a result, a low-lying 40^- terminating state can be formed with the proton contributing $(1/2)\hbar$ to the total spin, providing a straightforward interpretation of the experimental observations. Finally, a $m_i=-7/2$ proton hole leads to an aligned 43^- state, which is calculated to lie at a higher

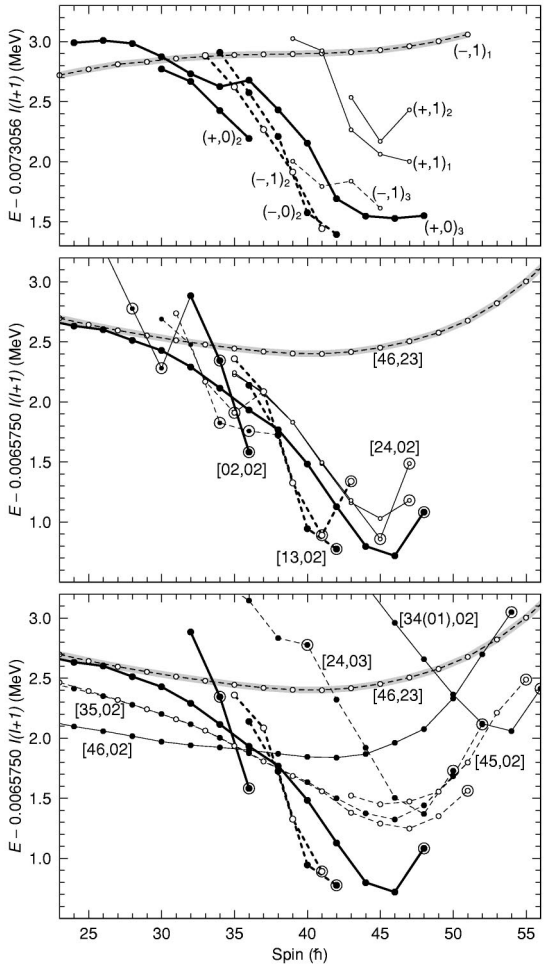

FIG. 4. Observed terminating bands of ^{154}Dy in the upper panel with their calculated counterparts in the middle panel. Note that the [13,02] label refers to the two bands terminating at 41^- (43^-) and 42^-, and [24,02] refers to the three bands terminating at 47^+ and 48^+. In the lower panel, some configurations predicted to terminate in the $I=(50-55)\hbar$ range are added. The bands are drawn versus the same reference as in Fig. 3 and the collective $(-,1)_1$ band and its theoretical counterpart are drawn in this figure (thick shaded line) to facilitate the comparison between the two types of configurations.

excitation energy. The level scheme of Fig. 1 contains a 43^- level, placed into a tentative $(-,1)_3$ ''band,'' which decays with a high-energy transition (1637 keV) to the terminating 41^- state, in agreement with the expectation. However, the 45^- level placed in this $(-,1)_3$ band, which is the only band member to decay via an $E2$ transition, cannot be formed in the [13,02] configurations under discussion and must therefore have another character. Possible interpretations for the latter state are discussed below.

It should be pointed out that one of the most striking experimental features of bands $(-,1)_2$ and $(-,0)_2$, i.e., the fact that they are connected by $M1$ transitions, finds a natural explanation within the present interpretation since the bands differ only by the signature of the $(g_{7/2}d_{5/2})$ proton hole. The occurrence of such $M1$ transitions close to termination was predicted in Ref. [1] and reiterated in Ref. [3], where two of them were first identified. Such bands of low collectivity, dominated by ''rotational-like'' $M1$ transitions, have recently attracted a lot of interest. It has been suggested that they correspond to a new rotational mode, the ''shears bands'' or ''magnetic rotation'' (see, e.g., [18]), for which some of the best examples can be found in neutron-deficient Pb nuclei [19]. The magnetic bands have been described in terms of the ''shears mechanism'' where the angular momentum is built from two ''blades,'' which start out at low-spin values as being aligned with the perpendicular and the symmetry axes, respectively. These blades close gradually when the angular momentum increases and becomes fully aligned in the terminating state [20]. Assuming that the present [13,02] configuration is prolate at intermediate spin values, the blades are built by the two $i_{13/2}$ neutrons aligned along the perpendicular axis and the $(g_{7/2}d_{5/2})$ proton hole, which is formed in the high-K [202]5/2 Nilsson orbital and thus aligned along the prolate symmetry axis. The other particles can then be considered as spectators gradually aligning along the rotation axis with increasing spin. Because of the relatively low rotational frequencies (small values of E_γ) in these $(-,1)_2$ and $(-,0)_2$ bands of ^{154}Dy, the closing of the blades will occur at relatively high angular momenta. Consequently, the $B(M1)$ values should remain large up to spin values fairly close to termination. These features suggest that bands $(-,1)_2$ and $(-,0)_2$ in ^{154}Dy may well represent the first instance where it has been possible to follow a shears-type configuration all the way to a high-spin termination.

2. Positive-parity levels

The description of terminating states with positive parity within the CNS approach is also rather successful. The lowest such level [36^+, band $(+,0)_2$] can be associated with the [02,02] configuration (Fig. 4), which has already been discussed in detail in Ref. [3]. The properties of this state are well reproduced, but the general trajectory of the [02,02] configuration in the energy vs spin plane deviates from the data. Therefore, the experimentally observed 34^+ state appears not to be related to the 34^+ state in the [02,02] configuration. A maximally aligned terminating state of 48^+ can be achieved for [24,02] configurations, providing a natural assignment for the highest level of band $(+,0)_3$. However, as can be seen in Fig. 4 (middle panel), positive-parity states with spin 44 and 46 are calculated to lie lower in energy once the rigid rotor reference is subtracted. In fact, since the 46^+ potential energy surface is extremely soft towards $\gamma=60°$, it may be argued that the [24,02] band should be considered to already terminate at 46^+. The smooth, gradual dependence of the experimental energy vs spin curve for band $(+,0)_3$ between $I=44\hbar$ and $48\hbar$, and the measured $B(E2)$ values [4] indicate that a substantial degree of collectivity persists up to the $I=46\hbar$ level, an observation in some disagreement with the calculations. These differences between calculations and experiment are even larger in Ref. [3], suggesting that the $g_{7/2}$ subshell should be even higher in energy than is the case with the present parametrization. States in bands $(+,1)_1$ and $(+,1)_2$ distinguish themselves from those in band $(+,0)_3$ through the odd spins. Within the [24,02] con-

figurations, such bands are naturally formed with both proton holes having the same signature. Thus, aligned 47^+ states can be formed either with both proton holes in $m_i=-5/2$ orbitals ($\alpha=-1/2$) or with one proton hole in $m_i=-7/2$ and the other in $m_i=-3/2$ ($\alpha=1/2$). The calculated bands are also given in the middle panel of Fig. 4. Again, the general trend is similar to that found in the data, but the computed excitation energies appear to be low by 0.5 MeV (relative to those of the structure terminating at 48^+).

3. Other possible terminating structures

Having identified terminating states up to $I=48^+$, it is interesting to also consider special band terminations that one may be able to observe at even higher spins in future measurements. Calculated configurations of this kind are drawn in the lower panel of Fig. 4 together with those identified unambiguously in the present work. Relative to the 46^+ or 48^+ levels from the [24,02] configuration, such states are most naturally formed by exciting an additional proton across the $Z=64$ gap or by lifting one neutron from the $(h_{9/2}f_{7/2})$ orbit to $i_{13/2}$ state. The resulting two signatures of the [35,02] configuration and the lowest signature of the [24,03] excitation give rise to terminating states with spins $I=50\hbar, 51\hbar$, and $52\hbar$ located on the yrast line or in its close proximity. The observed 45^- state of band $(-,1)_3$ can perhaps be assigned to this [35,02] configuration considering that the corresponding configuration has also been observed over an extended spin range, and tentatively to its termination at $I=58\hbar$, in the ^{156}Dy isotope [12,15]. In this ^{156}Dy nucleus, another configuration, with one more proton excited across the $Z=64$ gap [to a $(d_{3/2}s_{1/2})$ orbital], has been tentatively followed to termination at $I=62\hbar$. The corresponding [45,02] band in ^{154}Dy is also given in the lower panel of Fig. 4, with a termination in the yrast region at $I=55^-$. This [45,02] configuration could represent yet another possible interpretation for the 45^- state of band $(-,1)_3$. In any event, considering the decay properties in the $(-,1)_3$ band and the present discussion, it can be stated that the observed 43^- level probably corresponds to a mixture between the configurations discussed here. The [46,02] configuration discussed above is also relevant when searching for configurations terminating around $I=(50-55)\hbar$: this is clearly seen in the lower panel of Fig. 4. This configuration differs from the [45,02] one only by the fact that a sixth proton occupies a $h_{11/2}$ orbital rather than a $(d_{3/2}s_{1/2})$ state. At low spins, the [46,02] band is clearly lowest in energy, but the two configurations cross around $I=40\hbar$ after which the [45,02] band becomes lower by approximately 0.5 MeV for $I=(45-55)\hbar$. For spin values above $I=50\hbar$, the calculations suggest that configurations with one proton excited to the lowest $N=6$ $i_{13/2}$ orbital become competitive in energy, as illustrated by the [34(01),02] band in Fig. 4.

C. Shape coexistence in ^{154}Dy

In order to illustrate the well-developed shape coexistence present at high spin in ^{154}Dy, trajectories in the usual deformation space are presented for selected configurations in Fig. 5. It is worth keeping in mind that, in addition to the structures discussed here, a superdeformed band has also been reported in this nucleus [21]. The bands terminating at $I=36^+$, 41^-, and 42^- are calculated to lie very close to the noncollective $\gamma=60°$ axis, also for spins $(2-4)\hbar$ below termination. As a result these bands should have a very small collectivity. Therefore, it is not unexpected that only the general characteristics, but not the detailed properties, of these bands can be described by the CNS calculations. Although the trajectory of the [24,02] configuration through the deformation plane is more typical of a ''standard,'' terminating band, also in this case, the $I_{max}-2\hbar$ and $I_{max}-4\hbar$ states lie closer to the $\gamma=60°$ line than is the case for, e.g., the smooth terminating bands of the $A=110$ region [2]. The calculated shapes are in general agreement with the available lifetime data [4,5] showing very small $B(E2)$ reduced probabilities for the $36^+\rightarrow 34^+$ and $34^+\rightarrow 32^+$ decays in the $(+,0)_2$ band and substantially larger $B(E2)$ values for transitions close to the terminating $I=48^+$ state in band $(+,0)_3$. The [46,23] configuration is characterized by a prolate shape ($\varepsilon=0.22-0.25, \gamma\approx 0°$) up to the highest spin state (51^-) reported here. It would be interesting to follow this configuration to its calculated termination into a nearly spherical shape, high above the yrast line at $I=71^-$. Generally speaking, the deformation is larger at low spin as more protons are excited across the $Z=64$ gap, but the terminations tend to occur closer to a spherical shape. This feature is correlated with the relative slopes of the Nilsson orbitals for prolate and oblate shapes.

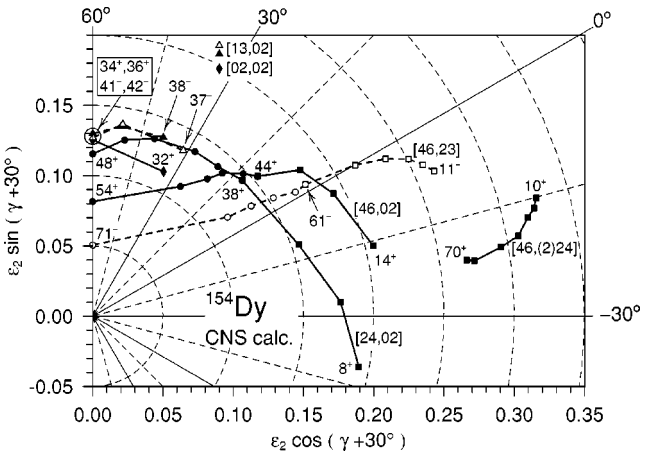

FIG. 5. Calculated deformations for some typical configurations in ^{154}Dy. The deformations are shown (by squares) in steps of $10\hbar$ at large collectivity and then for all spin values (by circles) in the spin range $[I_{\max}-10\hbar, I_{\max}]$. Note that the [46,23] configuration has only been observed at $I=51\hbar$, where it is still strongly collective, and that the $(+,0)_4$ band is interpreted as built either from the [46,(2)24] or [46,02] configuration.

V. SUMMARY

In summary, high-spin states up to $51\hbar$ have been established in the transitional nucleus ^{154}Dy. Some of the bands were found to maintain their smooth, collective rotational behavior up to the highest spins, while others were shown to terminate in the $I=(36-48)\hbar$ spin range. Configuration-

dependent cranked Nilsson-Strutinsky calculations are able to account for most of the observations. The collective bands are understood as being associated with neutron excitations across the $N=82$ shell gap. In contrast, the character of the terminations, abrupt or rather smooth, appears to be correlated to the number of protons excited across the $Z=64$ gap. Compared with previous studies of terminating bands in different mass regions, a much larger number of ''sidebands'' is observed in ^{154}Dy. The presence of these bands suggests that, with an increased experimental sensitivity, a very rich structure of interacting bands will be revealed in the unpaired, very high spin ($I \geqslant 50\hbar$) regime.

ACKNOWLEDGMENTS

This work was supported in part by U.S. DOE under Grants Nos. DE-FG02-95ER40939 (MSU), W-31-109-ENG-38 (ANL), DE-FG02-87ER40346 (Purdue University), and DE-FG05-88ER40407 (Vanderbilt University) and by the Swedish Natural Science Research Council.

[1] T. Bengtsson and I. Ragnarsson, Phys. Scr. T **5**, 165 (1983).
[2] A.V. Afanasjev, D.B. Fossan, G.J. Lane, and I. Ragnarsson, Phys. Rep. **322**, 1 (1999).
[3] H.W. Cranmer-Gordon *et al.*, Nucl. Phys. **A465**, 506 (1987).
[4] W.C. Ma *et al.*, Phys. Rev. Lett. **61**, 46 (1988).
[5] H. Hübel *et al.*, Prog. Part. Nucl. Phys. **28**, 295 (1992).
[6] W.C. Ma *et al.*, Phys. Rev. Lett. **84**, 5967 (2000), and references therein.
[7] I.-Y. Lee, Nucl. Phys. **A520**, 641c (1990).
[8] D.C. Radford, Nucl. Instrum. Methods Phys. Res. A **361**, 297 (1995).
[9] K.S. Krane, R.M. Steffen, and R.M. Wheeler, Nucl. Data Tables **11**, 351 (1973).
[10] M. Bergström, Plotwidgets Reference Manual, Niels Bohr Institute Internal Report, 1999.
[11] T. Bengtsson and I. Ragnarsson, Nucl. Phys. **A436**, 14 (1985).
[12] F.G. Kondev *et al.*, Phys. Lett. B **437**, 35 (1998).
[13] J. Simpson *et al.*, Phys. Lett. B **327**, 187 (1994).
[14] A.V. Afanasjev and I. Ragnarsson, Nucl. Phys. **A591**, 387 (1995).
[15] F. Saric, graduation thesis, Lund Institute of Technology, 2000 (unpublished); I. Ragnarsson and F. Saric (unpublished).
[16] I. Ragnarsson, Acta Phys. Pol. B **27**, 33 (1996).
[17] S.J. Gale *et al.*, J. Phys. G **21**, 193 (1995).
[18] S. Frauendorf, Z. Phys. A **358**, 163 (1997); Rev. Mod. Phys. (to be published).
[19] R.M. Clark and A.O. Macchiavelli, Nucl. Phys. **A682**, 415 (2001).
[20] I. Ragnarsson, in *Proceedings of the International Conference on the Nucleus: New Physics for the New Millenium, NAC, Faure, South Africa, 1999*, edited by F. D. Smit, R. Lindsay, and S. V. Förtsch (Kluwer Academic, Dordrecht, 2000), p. 347.
[21] D. Nisius *et al.*, Phys. Rev. C **51**, R1061 (1995).